Mechanical Fatigue in Repetitively Stretched Single Molecules of Titin

Miklós S. Z. Kellermayer,*† Steven B. Smith,‡ Carlos Bustamante,‡§ and Henk L. Granzier†

*Department of Biophysics, Pécs University Medical School, Pécs, H-7624 Hungary; †Department of Veterinary Comparative Anatomy, Pharmacology, and Physiology, Washington State University, Pullman, Washington 99164, and Departments of ‡Physics and §Molecular and Cell Biology, University of California, Berkeley, California 94720 USA

ABSTRACT Relaxed striated muscle cells exhibit mechanical fatigue when exposed to repeated stretch and release cycles. To understand the molecular basis of such mechanical fatigue, single molecules of the giant filamentous protein titin, which is the main determinant of sarcomeric elasticity, were repetitively stretched and released while their force response was characterized with optical tweezers. During repeated stretch-release cycles titin becomes mechanically worn out in a process we call molecular fatigue. The process is characterized by a progressive shift of the stretch-force curve toward increasing end-to-end lengths, indicating that repeated mechanical cycles increase titin's effective contour length. Molecular fatigue occurs only in a restricted force range (0–25 pN) during the initial part of the stretch half-cycle, whereas the rest of the force response is repeated from one mechanical cycle to the other. Protein-folding models fail to explain molecular fatigue on the basis of an incomplete refolding of titin's globular domains. Rather, the process apparently derives from the formation of labile nonspecific bonds cross-linking various sites along a pre-unfolded titin segment. Because titin's molecular fatigue occurs in a physiologically relevant force range, the process may play an important role in dynamically adjusting muscle's response to the recent history of mechanical perturbations.

INTRODUCTION

When a nonactivated (i.e., passive) striated muscle cell is stretched, passive force develops that restores muscle length following release. During active contraction passive force limits sarcomere-length inhomogeneity along the muscle cell and limits A-band asymmetry within the sarcomere (Horowits et al., 1986; Horowits and Podolsky, 1987). If the cell is exposed to repeated stretch and release cycles, the forces recorded during stretch are progressively shifted toward increasing sarcomere lengths, indicating that, with time, the cell becomes mechanically worn out (Granzier and Wang, 1993b; Helmes et al., 1999). When a relaxed muscle cell is stretched rapidly to a given sarcomere length, passive force decays as a function of time (Horowits, 1992; Linke et al., 1994) in a process known as stress relaxation. Mechanical fatigue and stress relaxation probably derive from the same mechanism: time- therefore rate-dependent reorganization in the structures that determine passive muscle force. The significance of time-dependent changes in passive muscle behavior is not fully understood. In cardiac myocytes that physiologically go through repeated contractile cycles, passive mechanical fatigue may be particularly relevant (Helmes et al., 1999).

One of the main determinants of passive muscle force is the filamentous intrasarcomeric protein titin (Granzier and Irving, 1995). Titin is an ~3.5-million-dalton protein (cf. Gregorio et al., 1999; Maruyama, 1997; Trinick and Tskhovrebova, 1999; Wang, 1996) that spans the half-sarcomere, from the Z- to the M-line (Fürst et al., 1988; Labeit and Kolmerer, 1995). It is anchored to the Z- and M-lines and is strongly attached to the thick filaments of the A-band. The I-band segment of the molecule is constructed of serially linked immunoglobulin (Ig)-like domains interspersed with unique sequences including a proline (P)-, glutamate (E)-, valine (V)-, and lysine (K)-rich (PEVK) domain (Labeit and Kolmerer, 1995). Upon stretch of the sarcomere, passive tension is generated by the extension of titin's I-band segment (Trombitás et al., 1995; Granzier et al., 1996; Linke et al., 1996). The A-band segment is composed primarily of super-repeats of different Ig- and fibronectin (FN3)-like domains (D zone and C zone super-repeats) and less regular regions that connect to the M-line and I-band segments (Labeit and Kolmerer, 1995). The A-band segment does not participate in the generation of passive force under physiological conditions. Rather, this portion appears to provide a structural scaffold for thick-filament assembly (Trinick, 1996).

The mechanical properties of titin have been explored in recent single-molecule manipulation experiments, revealing that the molecule behaves as an entropic spring in which unfolding of the globular domains occurs at high force during stretch (Kellermayer et al., 1997; Rief et al., 1997; Tskhovrebova et al., 1997) and refolding at low force during release (Kellermayer et al., 1997). During repeated stretch-release cycles the stretch force curve moved progressively toward the release curve, indicating that titin, similarly to relaxed muscle, can be mechanically worn out (Kellermayer et al., 1997, 1998). Furthermore, when a titin molecule is rapidly stretched to and held at a given length, force relaxes as a function of time in a stepwise fashion, where the steps can be correlated with contour-length increments by individual domain unfolding events (Tskhovrebova et al.,

Received for publication 4 August 2000 and in final form 14 November 2000.

Address reprint requests to Dr. Miklós S. Z. Kellermayer, Department of Biophysics, Pécs University Medical School, Szigeti ut 12, Pécs, H-7624 Hungary. Tel.: 36-72-536-271; Fax: 36-72-536-261; E-mail: kmiklos@apacs.pote.hu.

0006-3495/01/02/852/12 $2.00

1997). It is possible that mechanical wear-out is related to the kinetics of domain folding-unfolding and that during the repeated mechanical cycles an increasingly larger number of domains failed to refold, leaving behind a progressively longer pre-unfolded titin segment. However, as domain unfolding is unlikely to occur in titin during each contraction cycle under physiologically relevant forces and sarcomere lengths (Trombitás et al., 1998), domain unfolding-refolding kinetics are unlikely to be the sole determinants of the wear-out process.

To explore the mechanisms behind titin's mechanical wear-out, single molecules were repetitively stretched here by using force-measuring optical tweezers (Smith et al., 1996; Kellermayer et al., 1997), and the data were compared with theoretical predictions based on the elastic behavior of serially linked wormlike chains (WLCs) (Bustamante et al., 1994; Marko and Siggia, 1995). We show that titin's mechanical wear-out, named here molecular fatigue, is restricted to the low-force regime (0 to ~25 pN) at the employed rates of stretch (40–100 nm/s). We propose that molecular fatigue involves a rate-dependent process in which nonspecific, labile bonds that cross-link, and thereby shorten, the chain gradually rupture upon stretch and that these bonds do not re-form completely before the immediately following stretch cycle. Because the low-force regime corresponds to the range of forces generated under physiological circumstances, titin's molecular fatigue may play a role in modulating the passive mechanical behavior of striated muscle.

MATERIALS AND METHODS

Protein preparation

Titin was prepared from striated muscle using previously established protocols (Kellermayer and Granzier, 1996; Soteriou et al., 1993) with modifications. Various muscle sources were used, including rabbit longissimus dorsi, soleus, and cardiac and rat cardiac muscles. Similar results were obtained for the titins prepared from different muscle species. Titin purified by gel filtration was used in our experiments (0.8 × 90 cm Sepharose CL-2B column equilibrated with CB solution: 30 mM potassium phosphate, pH 7.0, 0.6 M KCl, 0.1 mM EGTA, 0.3 mM dithiothreitol (DTT), 2 μg/ml leupeptin, 1 μM *trans*-epoxysuccinyl-L-leucylamido-(4-guanidino)butane (E-64), 0.01% NaN_3, 0.05% Tween-20). Samples were stored on ice in CB in the presence of 0.1% NaN_3, 40 μg/ml leupeptin, and 20 μM E-64. According to electrophoretic analysis (Granzier and Wang, 1993a), titin was stable on ice for weeks.

Mechanical manipulation of titin

For single-molecule manipulation, titin was repetitively stretched by using a counter-propagating dual-beam optical tweezers instrument capable of generating and measuring forces up to ~160 pN, twice as large as in our previous work (Kellermayer et al., 1997). Titin was mounted on microspheres and mechanically stretched as reported previously (Kellermayer et al., 1997). The Z-line end was attached to a T12 anti-titin-coated, 3.18-μm carboxylated latex bead (SpheroTech, Libertyville, IL) captured in the optical trap. The T12-coated latex beads were blocked with 1% BSA and 0.2% Tween-20 before coating them with titin, to inhibit nonspecific binding. The M-line end of titin was attached to a 2.5-μm amino-modified silica bead (Bangs Laboratories, Fishers, IN) coated with the photoreactive cross-linker sulfo-succinimidyl 6-(-4′azido-2′-nitrophenylamino)hexanoate (sulfo-SANPAH), as described previously (Kellermayer et al., 1997). The photoreactive cross-linking provided non-sequence-specific attachment of the bead to titin. As a result, the length of the captured A-band segment was variable from experiment to experiment. In some experiments amino-modified latex beads were used instead of silica. These latex beads gave identical results to those obtained with the silica beads. The cross-linking reaction was initiated by exposing the silica (or latex) bead, held with a moveable glass micropipette, to the optical trap-forming laser beam. Once a permanent attachment was established, titin was allowed to rest for 5 min before the beginning of mechanical experiments. The molecule was stretched by moving the micropipette away from the trap at a constant rate (typical rates, ~40–100 nm/s) until a maximum predetermined force (f_{max}) was reached (typical f_{max}, ~160 pN). Then the process was reversed to obtain the release half-cycle. For repetitive stretch and release, the mechanical cycles continued without pause between the cycles. Force acting on the trapped bead was measured from the difference in the momentum between the light entering and exiting the trap (Smith et al., 1996). The length of titin was obtained from the distance between the centroids of the bead images corrected with the beads' radii. The stretch-release experiments were carried out in assay buffer (AB solution: 25 mM imidazole-HCl, pH 7.4, 0.2 M KCl, 4 mM $MgCl_2$, 1 mM EGTA, 0.01% NaN_3, 1 mM DTT, 20 μg/ml leupeptin, 10 μM E-64). For stretching chemically denatured titin, 4 M guanidine hydrochloride (GdnHCl) in AB solution was introduced in the flow chamber by gravity feeding from a reservoir while holding a molecule between the two beads (one in the trap and the other held by the micropipette). The arrival of the 4 M GdnHCl solution was detected by the defocusing of the microscopic image due to the change in the solution's index of refraction (n_s). Chemically denatured titin was stretched following a 5-min waiting period and refocusing to obtain sharp bead images for position measurement. Because force determination did not rely on calibration schemes, refocusing and the change in n_s did not affect the force measurement. From the release force data the apparent persistence length of the tether was calculated and compared with previously obtained persistence-length statistics (Kellermayer et al., 1997, 2000) to calculate the number of molecules in the tether. Subsequently, the force data were normalized to the single molecule (see below). Considering that mounting a titin tether between the two microspheres involved varying degrees of mechanical agitation of the tether, here we define the first stretch-release cycle as one following a ≥5-min rest period in the shortened state. Accordingly, it was possible to carry out more than one first stretch-release cycle on the same tether (see Fig. 1 *b*). In such experiments the rest period preceded each first mechanical cycle.

Assessment of nonspecific titin-microsphere interaction

The nonspecific binding of titin to microspheres was measured by monitoring, with two different methods, the amount of fluorescently labeled titin attached to the surface of the spheres. Titin, purified from rabbit longissimus dorsi was labeled overnight on ice with 400X molar excess of tetramethylrhodamine-5-(and -6)-iodoacetamide (TMRIA) in AB. Unbound fluorophores were removed by extensive dialysis against AB. The 3.18-μm carboxylated latex microspheres (SpheroTech, Libertyville, IL) at a concentration of 0.05% (w/v) were incubated on a rotorack (30 min at room temperature) in the presence of fluorescently labeled titin (25 μg/ml) in AB solution or in 4 M GdnHCl. To examine the effect of blocking with bovine serum albumin (BSA) and Tween-20 (see above), pre-blocked microspheres were used. Unbound protein was removed by centrifugation (5000 rpm, 5 min) and resuspension in AB. In the case of 4 M GdnHCl, which has a density greater than that of latex (precluding microsphere sedimentation), following the incubation step the microsphere suspension

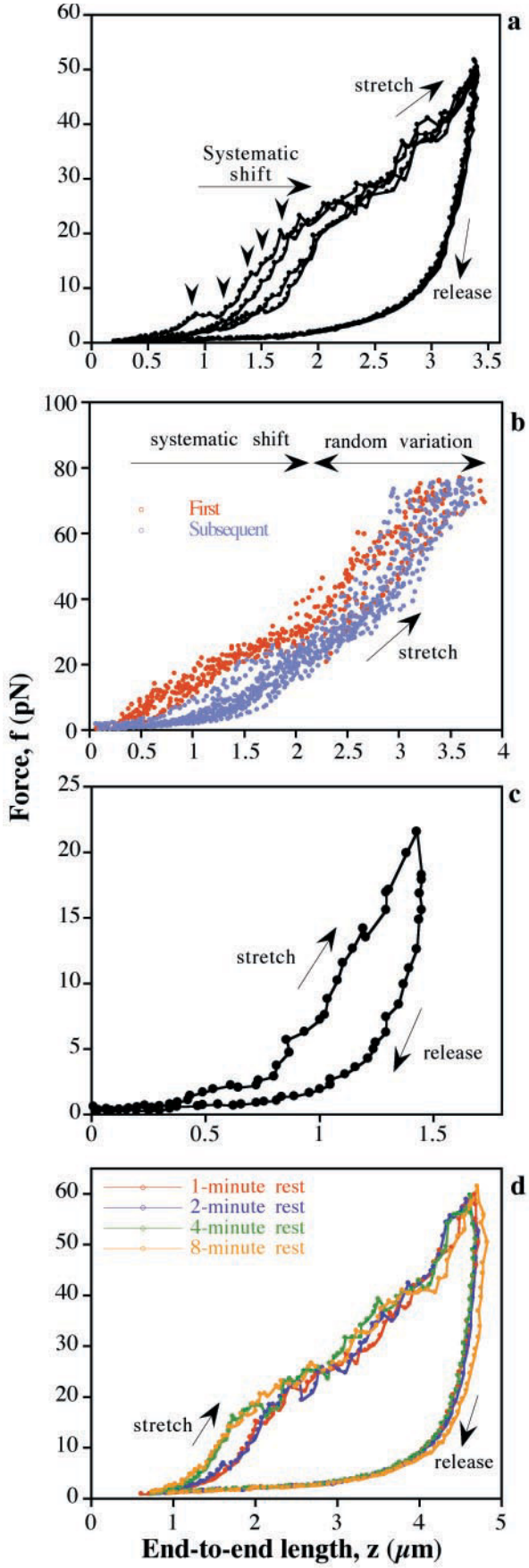

was first diluted with AB (threefold), and then we proceeded with the centrifugation and resuspension steps.

Titin nonspecifically adsorbed to the microsphere surface was quantified by measuring the fluorescence intensity distribution for a bulk sample of microspheres by using a fluorescence-activated cell sorter (FACSCalibur, Becton Dickinson, San Jose, CA). The microsphere suspension was diluted 100-fold with AB solution. A total of 10,000 beads were counted for each sample using an excitation wavelength of 488 nm. For each microsphere the fluorescence intensity and the forward scatter (11°) were measured.

The number of fluorescently labeled titin molecules nonspecifically adsorbed to the microsphere surface was counted on confocal microscopic images (MRC-1024 laser scanning confocal microscope, Bio-Rad Laboratories, Hertfordshire, UK). Optical sections of titin-coated microspheres were acquired in 0.05–0.1-μm z axis steps. The images were imported into Image software (v.1.61, Wayne Rasband, National Institutes of Health, Bethesda, MD) running on a Power Macintosh G3 computer and analyzed with custom-written macros. To count the number of titin molecules on the entire surface of a bead, three-dimensional projection of the stack of optical sections was carried out.

Muscle fiber mechanics

Single muscle fibers dissected from human m. soleus (biopsies obtained in accordance with the protocol "Role of Titin in Human Muscle Tissue 2" (Washington State University) were mechanically and chemically skinned. The fibers were kept in relaxing solution containing high concentrations of protease inhibitors and were used within 48 h of harvest. For a detailed description of the solution composition and muscle-fiber mechanics, see Ogut et al., 1999. Briefly, the ends of the fiber were wrapped around fine pins (100-μm diameter) that were glued to the motor and the force transducer. To limit stretching of the fiber ends, a small volume (<1 μl) of 2% glutaraldehyde solution was applied to the portions of the fiber wrapped around the pins (Chase and Kushmerick, 1988). Sarcomere length (SL) was obtained by using laser diffraction. To measure the passive force versus SL relation, relaxed fibers were slowly stretched (35 nm/s per sarcomere) from their slack SL to a predetermined amplitude, followed by release back to the slack length. To calculate the force generated in a single titin molecule, the measured forces were normalized with the number of titin molecules in the cross-sectional area of the muscle fiber (Granzier and Irving, 1995). The muscle fiber cross-sectional area was calculated from the axes of its elliptic image recorded using phase-contrast microscopy (Granzier and Irving, 1995). The number of titin molecules in the cross-sectional area was then calculated by assuming 70% occupancy of the cross

FIGURE 1 Force versus end-to-end length curves of titin molecules obtained during repetitive stretch-release cycles. Arrows indicate direction of data acquisition (stretch or release). (*a*) Four successive stretch-release cycles. Arrowheads indicate abrupt force changes. Below ~25 pN, the force curves shift to progressively longer end-to-end lengths with the number of stretch-release cycles. Stretch rate, 98 nm/s. (*b*) Superimposition of 7 first (red) and 12 subsequent (i.e., second and third cycle) (blue) stretch data (combined data from two different tethers of similar length). See text for our criterion of first stretch-release cycle. The variation between the first and subsequent stretches is random above ~25 pN but involves a systematic shift below ~25 pN. Stretch rate, 44 nm/s. (*c*) The f versus z curve of titin stretched to $f_{max} < 25$ pN. Stretch rate, 35 nm/s. (*d*) Dependence of the force response on the length of rest period between the first and subsequent stretch-release cycle. The initial force response (at $f <$ 25 pN) is recovered following a rest period of $\geq$4 min. Stretch rate, 42 nm/s. Data shown here are normalized for the single molecule, obtained by halving the raw force data that apparently came from a titin doublet (see Materials and Methods).

section by myofibrils (Eisenberg, 1983), 540 thick filaments per μm^2 myofibril cross-sectional area (Granzier and Irving, 1995), and six titins per thick filament (Cazorla et al., 2000).

Theory and calculations

Force data were fitted with the WLC equation (Bustamante et al., 1994; Marko and Siggia, 1995):

$$\frac{fA}{k_BT} = \frac{z}{L} + \frac{1}{4(1 - z/L)^2} - \frac{1}{4}, \quad (1)$$

where f is force, A is persistence length, z is end-to-end length, L is contour length, k_B is Boltzmann's constant, and T is absolute temperature. At high fractional extension (z/L), as z approaches L, the inverse square term of Eq. 1 dominates. Accordingly, at high extensions, $f^{-1/2}$ varies linearly with z as

$$f^{-1/2} = -\frac{2}{L}(A/k_BT)^{1/2}z + 2(A/k_BT)^{1/2}. \quad (2)$$

Extrapolation of this linear function to the abscissa, where $f^{-1/2} = 0$, provides the contour length. The y-($f^{-1/2}$)-axis intercept, on the other hand, allows the apparent persistence length of the titin tether to be calculated as

$$A = \frac{k_BT}{4f_{\text{intercept}}}. \quad (3)$$

The persistence length of the single titin molecule ($A_0 \approx 1.6$ nm) has been obtained from the statistical distribution of A derived from many stretch-release experiments (Kellermayer et al., 1997, 2000). Considering that for multi-molecular tethers force at a given fractional extension is the integer multiple of the single-molecule force, using A_0 the number of molecules in any titin tether was calculated from A derived from the experimental force-extension curve as

$$n = \frac{A_0}{A}. \quad (4)$$

Raw force was normalized to the single molecule according to the number of molecules in the tether as

$$f_{\text{normalized}} = f/n. \quad (5)$$

Force versus end-to-end length curves for partially unfolded titin were generated with the following theoretical considerations. As a titin molecule is mechanically stretched and becomes gradually unfolded, its contour length exceeds that of the native molecule (~1 μm (Nave et al., 1989)) and approaches the length of titin's primary structure (~10 μm (Labeit and Kolmerer, 1995)). In addition, the apparent persistence length (A) of titin decreases as the rigid folded, native molecule ($A_{\text{folded}} \approx 15$ nm (Higuchi et al., 1993)) is converted into the flexible unfolded ($A_{\text{unfolded}} \approx 1.6$ nm (Kellermayer et al., 2000)). Accordingly, if the molecule is stretched in successive mechanical cycles to progressively increasing lengths, the release $f^{-1/2}$ versus z curves will extrapolate to progressively increasing contour lengths and progressively decreasing ($f^{-1/2}$)-axis intercepts. As a result, the extrapolated $f^{-1/2}$ versus z curves of a progressively unfolded titin molecule intersect off-axis, so that the coordinates of the intersection are ($z > 0, f^{-1/2} > 0$). The coordinates of the intersection can be numerically derived from the completely folded and completely unfolded boundary states. By solving for the end-to-end length at the intersection (z^*) we obtain

$$z^* = \frac{L_u(A_u^{1/2} - A_f^{1/2})}{A_u^{1/2} - R_L A_f^{1/2}}, \quad (6)$$

where L_u is the contour length of completely unfolded titin, A_u and A_f are the persistence lengths of the unfolded and folded molecule, respectively, and R_L is the ratio of the unfolded and folded contour lengths (L_u/L_f). By substituting z^* into Eq. 2 we obtain the force at the intersection (f^*) as

$$f^* = \frac{k_BT}{4A_u\left(1 - \frac{A_u^{1/2} - A_f^{1/2}}{A_u^{1/2} - R_L A_f^{1/2}}\right)^2}. \quad (7)$$

In deriving Eq. 7 above, the parameters of the completely unfolded molecule were used (where $A = A_u$ and $L = L_u$) for the sake of simplicity, but equivalent results can be obtained for the completely or partially unfolded states as well. To numerically test for the presence of intersection between the extrapolated $f^{-1/2}$ versus z curves of partially unfolded titin, WLC curves were generated by using Eq. 1 with the consideration that the folded and unfolded segments of the molecule are serially linked and therefore bear equal force. Fractional extension (z/L) of both the unfolded ($A_u = 1.6$ nm) and folded ($A_f = 15$ nm) segments were calculated for a given force and multiplied with their respective contour lengths (varied according to the degree of unfolding) to obtain their end-to-end lengths. The end-to-end length of the entire titin molecule for the given force was obtained by combining the end-to-end lengths of the unfolded and folded segments.

Modeling and simulation

Monte Carlo simulations were carried out to model domain unfolding/refolding and nonspecific bond rupture/formation in titin under force based on previously used simulation algorithms (Kellermayer et al., 1997, 2000). The model molecule contained 70 globular domains and a 760-nm-long pre-unfolded segment analogous to the skeletal-muscle PEVK segment (2000 residues × 0.38 nm (Labeit and Kolmerer, 1995)), whose apparent contour length is shortened by the presence of cross-links between sites along the segment (1400 sites corresponding to the approximate number of charged residues in PEVK (Labeit and Kolmerer, 1995)). The transition length (Δx) and the enclosed loop perimeter (see Results) were randomly generated between 0.3–0.8 nm (Bell, 1978) and 1–3 nm (up to two persistence-length distance), respectively. As the chain was extended, force was generated according to the WLC equation (Bustamante et al., 1994; Marko and Siggia, 1995). At each step, for the given force, the number of bonds ruptured and domains unfolded/refolded were calculated according to Bell (1978) and Evans and Ritchie (1997):

$$dN = N\omega_0 dt e^{-(E_a - f\Delta x)/k_BT}, \quad (8)$$

where dN is the number of bonds broken or domains unfolded/refolded during the dt polling interval, and N is the number of available bonds or folded domains. The value of ω_0 was 10^8 (Bell, 1978), k_BT 4.14 pNnm, and E_a 28 pNnm. The value of Δx was 0.3 nm for unfolding (Kellermayer et al., 1997; Rief et al., 1997, 1998) and 8 nm for refolding (Kellermayer et al., 1997), and for the noncovalent cross-link the longest Δx was selected from an array of available cross-links. In case of fractional dN, the process was permitted or prohibited depending on a comparison with a number generated randomly between 0 and 1. Unfolding or refolding events incremented or decremented the chain length with 28 nm. Bond rupture events incremented the chain length with the randomly selected loop perimeter. Bond re-formation was allowed to proceed only at forces below 2 pN according to the number of available counter binding sites (N_1 and N_2) and the rate constant of bond formation (k_+), according to a second-order reaction (Bell, 1978):

$$dN_b/dt = k_+N_1N_2. \quad (9)$$

A rate constant of $k_+ = 10^{-5}$ s^{-1} was used, calculated as

$$k_+ = (t_{1/2}N_0)^{-1}, \quad (10)$$

where $t_{1/2}$ is the half-life of the reaction (estimated ~2 min, see Fig. 1 *d*) and N_0 is the total initial number of bond-forming sites. Each bond formation event decremented the chain length with a randomly generated loop perimeter. The simulations were carried out by using Object Pascal (Metrowerks CodeWarrior v.10) on an Apple PowerMacintosh G3 computer.

Chemicals

All chemicals were reagent grade. Leupeptin and E-64 were obtained from Peptides International (Louisville, KY), sulfo-SANPAH from Pierce Chemical Co. (Rockford, IL), and TMRIA (mixed isomers) from Molecular Probes (Eugene, OR). All other chemicals were purchased from Sigma Chemical Co. (St. Louis, MO).

RESULTS

Mechanical fatigue in single titin molecules

The force versus end-to-end length (*f* versus *z*) curves of a titin molecule obtained in four consecutive stretch-release cycles (Fig. 1 *a*) illustrate the characteristics of titin exposed to repetitive stress. In each cycle, force begins to rise nonlinearly upon stretch, and the molecular length approaches a limit determined by the contour length of the native titin molecule that consists of folded globular domains and the PEVK and other unique sequence elements. At ~25 pN, a characteristic stretch transition begins that corresponds to the unfolding of titin's globular domains (Kellermayer et al., 1997; Rief et al., 1997; Tskhovrebova et al., 1997). Even below ~25 pN, however, transitions variably and intermittently appear (arrowheads, Fig. 1 *a*). Above ~25 pN, force rises monotonically as the stretch transition continues to take place until the maximal experimental force, f_{max} is reached. During release the force data of each consecutive stretch-release cycle trace the same curve (Fig. 1 *a*), which is a WLC curve at the intermediate and high forces (Kellermayer et al., 1997, 1998).

During repeated stretch-release cycles, at forces below ~25 pN the stretch curves were systematically shifted with each cycle toward increasing lengths (Fig. 1 *b*). At forces above ~25 pN, however, for a given end-to-end length, only random force variation occurred between the first and subsequent stretch-release cycles (Fig. 1 *b*). The systematic shift of the force curves toward increasing lengths indicates that titin became mechanically worn out in a kinetic process that takes place at forces <25 pN. If titin is stretched to f_{max} < 25 pN (Fig. 1 *c*), force hysteresis appears, indicating that the molecule is not in conformational equilibrium in this low-force regime.

Although mechanical fatigue occurs in titin in repeated stretch-release cycles, the molecule recovers following rest in the fully or partially shortened state. Mechanical recovery is facilitated by increasing the time spent in the contracted configuration (Fig. 1 *d*), and complete recovery is achieved on the minutes time scale (~4 min).

Mechanical fatigue in relaxed single muscle fibers

To explore the physiological significance of our observations, the force-response of single titin molecules was compared with that of single relaxed soleus muscle fibers. Scaling the muscle-fiber forces with the number of titin molecules in the muscle cross-sectional area down to the single titin molecule revealed that mechanical fatigue also occurs in situ, in the low-force range (<25 pN; Fig. 2).

Titin as serially linked chain of folded and unfolded segments

The mechanical behavior of progressively unfolded titin was explored numerically and experimentally (Fig. 3). Titin behaves as a WLC whose elasticity is described in terms of its persistence length (*A*), and its end-to-end length approaches the contour length as the molecule is stretched to high forces (see Materials and Methods). In our numerical model, unfolding increases the contour length of titin from 1 μm of the completely folded (Nave et al., 1989) to ~10 μm of the completely unfolded (Labeit and Kolmerer, 1995) molecule (Fig. 3 *a*). In addition, the apparent persistence length decreases from ~15 nm of the completely folded chain (Higuchi et al., 1993) to ~1.6 nm of the completely unfolded chain (Kellermayer et al., 2000). As Fig. 3 *a* indicates, the extrapolated linear regions of the $f^{-1/2}$ versus *z* curves for all unfolded/folded ratios have a common intersection (crossover point) whose offset (where $z >$ and $f^{-1/2} > 0$) from the length and force axes are determined by the folded/unfolded contour-length and persis-

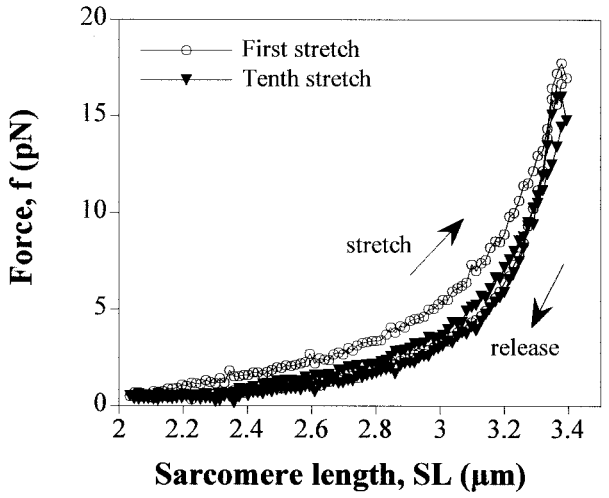

FIGURE 2 Force versus sarcomere length curves of human soleus muscle fiber obtained in repetitive stretch-release cycles. The force data are normalized to the single titin molecule by calculating the number of thick filaments in the fiber's cross section and assuming six titins/thick filament (Granzier and Irving; 1995 (see Materials and Methods). Arrows indicate direction of data acquisition (stretch or release).

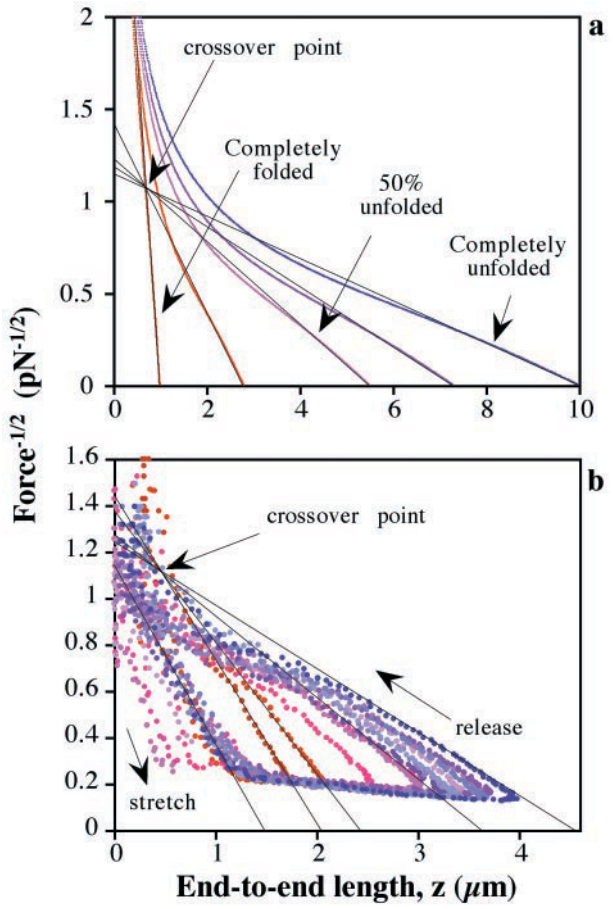

FIGURE 3 Analysis of the wormlike chain (WLC) behavior of partially unfolded titin. (*a*) Force$^{-1/2}$ ($f^{-1/2}$) versus end-to-end length (z) representation of theoretical WLC curves of completely folded and 20%, 50%, 70%, and 100% unfolded titin. The high-extension segment of the WLC curves extrapolate to progressively increasing contour lengths and reveal progressively decreasing apparent persistence lengths as a function of increasing unfolded/folded ratio. The linear fits to the high-force regime contain an off-axis common intersection (crossover point). Theoretical WLC curves were generated according to the WLC equation (Eq. 1) using 1- and 10-μm contour lengths and 15- and 1.6-nm persistence lengths for the folded and the unfolded titin chain, respectively (see Materials and Methods). (*b*) Experimental $f^{-1/2}$ versus z curves of a titin molecule stretched to progressively increasing lengths. Progression from the 1st to the 13th mechanical cycle is indicated with a color transition from dark red to dark blue. Extrapolated linear fits to the release force data contain an off-axis common intersection (crossover point). By contrast, the extrapolated linear, apparent WLC segment in the stretch data do not contain the same intersection, but intersect the force axis at points corresponding to persistence lengths shorter than that of the unfolded chain. Stretch rate, 49 nm/s. Arrows indicate direction of data acquisition (stretch or release).

tence-length ratios, respectively (see Materials and Methods). Experimental data obtained from the release curves of titin stretched to progressively increasing end-to-end lengths, hence to increasing unfolded/folded ratios, reproduced the off-axis common intersection (Fig. 3 *b*). By contrast, the extrapolated linear fit to the WLC region in the stretch $f^{-1/2}$ versus z data failed to pass through the common intersection (Fig. 3 *b*). Rather, the stretch WLC behavior corresponds to a highly flexible chain with short apparent persistence length (~0.2–1.0 nm). However, because titin is not in conformational equilibrium in the low-force range (~0–25 pN), as indicated by the presence of force hysteresis (Fig. 1 *c*), the apparent, highly flexible WLC behavior is probably caused by transitions through kinetic intermediates that are shorter than titin's available contour length.

Sources of titin's mechanical fatigue

Kinetic intermediates shorter than the available contour length may arise from two possible sources: 1) intramolecular interactions or cross-links between various sites along the molecule and 2) interactions between titin and the microspheres that may artificially result in contour-length reduction. Nonspecific titin-microsphere interaction was assessed by two methods: 1) titin was stretched in the presence of the chemical denaturant GdnHCl that abolishes intramolecular bonds but may not necessarily inhibit the titin-microsphere binding (Fig. 4) and 2) the nonspecific binding of fluorescently labeled titin to latex microspheres was directly measured with confocal microscopy and FACS analysis (Fig. 5). The presence of 4 M GdnHCl completely abolished titin's mechanical fatigue (Fig. 4, *a* and *b*). Mechanical fatigue was restored, however, upon washing GdnHCl out (Fig. 4 *c*). When latex microspheres in AB solution were incubated with fluorescently labeled titin, the molecules bound nonspecifically to the beads (16.6 molecules/bead ± 6.1 SD; Fig. 5, *a* and *d*). Similarly, nonspecific titin binding was present in 4 M GdnHCl (20.1 molecules/bead ± 6.2 SD; Fig. 5, *b* and *d*), suggesting that GdnHCl did not interfere with the binding of titin to the microsphere surface. The nonspecific binding of titin to the beads was abolished by pretreating the beads with 1% BSA and 0.2% Tween-20 (Fig. 5, *c* and *d*). The FACS analysis results supported the confocal microscopic observations (Fig. 5 *e*): although titin nonspecifically bound to the latex microspheres even in the presence of 4 M GdnHCl, preblocking the beads resulted in an order-of-magnitude reduction in fluorescence. Thus, bead-protein interactions are unlikely explanations for the observed mechanical wear-out. Rather, intramolecular processes are responsible for the appearance of titin's mechanical fatigue.

Simulation of titin's mechanical fatigue with nonspecific intra-chain bond kinetics

Mechanical fatigue in titin was modeled by superimposing the rupture/formation kinetics of labile intra-chain cross-links on the molecule's WLC behavior. The kinetic intermediates seen during stretch (Fig. 3 *b*) were assumed to represent conformational states in which nonspecific, noncovalent bonds cross-link different sites along a pre-un-

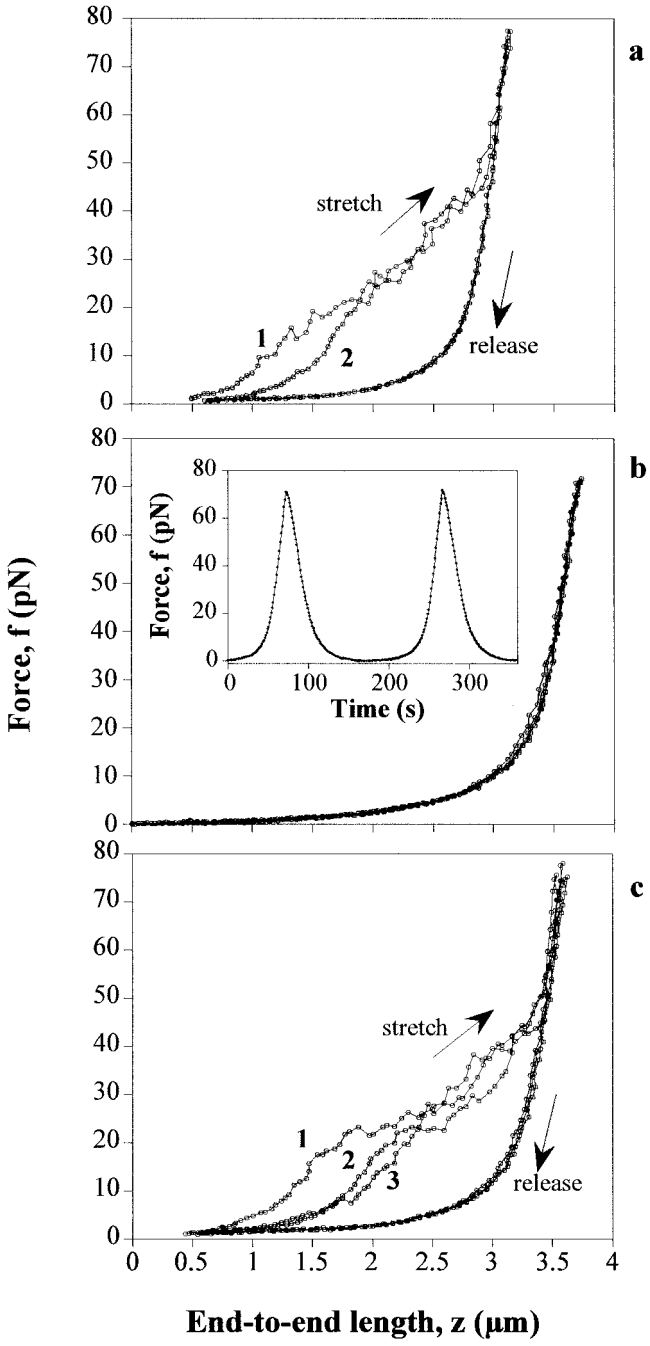

FIGURE 4 Effect of 4 M GdnHCl on the mechanical behavior of titin. The *f* versus *z* curves were obtained in consecutive stretch-release cycles before the addition of (*a*), in the presence of (*b*), and following the washout of (*c*) the denaturant. Arrows indicate direction of data acquisition (stretch or release). The inset in *b* shows the stretch-release protocol, indicating that the plot contains data from two successive mechanical cycles. Data for the same titin tether are displayed in the panel, normalized for the single molecule, obtained by halving the raw force data that apparently came from a titin doublet (see Materials and Methods). The reversible force curve above ~50 pN indicates that complete mechanical unfolding of titin occurred (Kellermayer et al., 1998), in contrast to other titin tethers shown in this work that were stretched with similar forces and to similar lengths (see Fig. 1). The low, ~50-pN force at the onset of the reversible portion of the force curve suggests that only a segment of titin containing a few folded segment in titin. The bonds shorten the effective contour length of this segment by interconnecting bond-forming sites along its contour. The simplest model has the molecular portion enclosed by a cross-link in the form of a loop. The contour length of the molecule is decremented by each bond with a distance equal to the perimeter of the enclosed loop. As titin is stretched, force is generated in the chain, which leads to the rupture of these nonspecific bonds. The intermittent, variable transitions seen during the early phase of stretch may correspond to such bond rupture events (Fig. 1 *a*, arrowheads). Under external force, the frequency (ν) of bond rupture can be expressed as

$$\nu = N_b \omega_0 e^{-(E_a - f\Delta x)/k_B T}, \quad (11)$$

where N_b is the number of available bonds, ω_0 is the natural vibration frequency of the bond in vacuum, E_a is the bond energy, f is the force acting along the reaction coordinate, and Δx is a characteristic distance (along the reaction coordinate) associated with the transition state for bond breaking (Bell, 1978; Evans and Ritchie, 1997). Thus, the energy barrier of bond rupture is decreased by the external force depending on the displacement (Δx) it induces along the molecular axis. Δx, however, varies along the chain and depends on the structural and energy landscape of each binding site (Kazmirski and Daggett, 1998; Merkel et al., 1999). Because each cross-link in the chain bears the same force, the cross-link with the longest Δx will tend to rupture first at the given force. Therefore, external force polls the chain for the longest Δx. Each bond rupture event increments the chain contour length with the perimeter of the enclosed loop. Because realistic stretch rates exceed the equilibrium bond rupture rate, the process occurs at forces greater than the equilibrium force. By contrast, the cross-links re-form in a diffusion-limited process only if the chain spends sufficient time in the shortened, low-force state (at slack length) so that the bond-forming sites can encounter each other. The rate of the nonspecific bond formation (dN_b/dt) can be expressed with Eq. 9 as a second-order reaction. Even a moderate increase in the end-to-end length inhibits the formation of the bonds by diluting the number of sites that participate in bond formation. Because the stretch and release rates exceed the rates of bond rupture and re-formation, respectively, force hysteresis appears even at low forces (<25 pN), where domain unfolding does not yet occur at the employed experimental stretch rate (Fig. 1 *c*). A Monte Carlo simulation based on our model reproduced all the essential features of our data including molecular fatigue at low forces (<25 pN) during successive stretch-release cycles (Fig. 6 *a*), the apparent, highly flexi-

unstable globular domains were captured between the microspheres. The presence of molecular fatigue suggests that the process is independent from the number and stability of globular domains in titin.

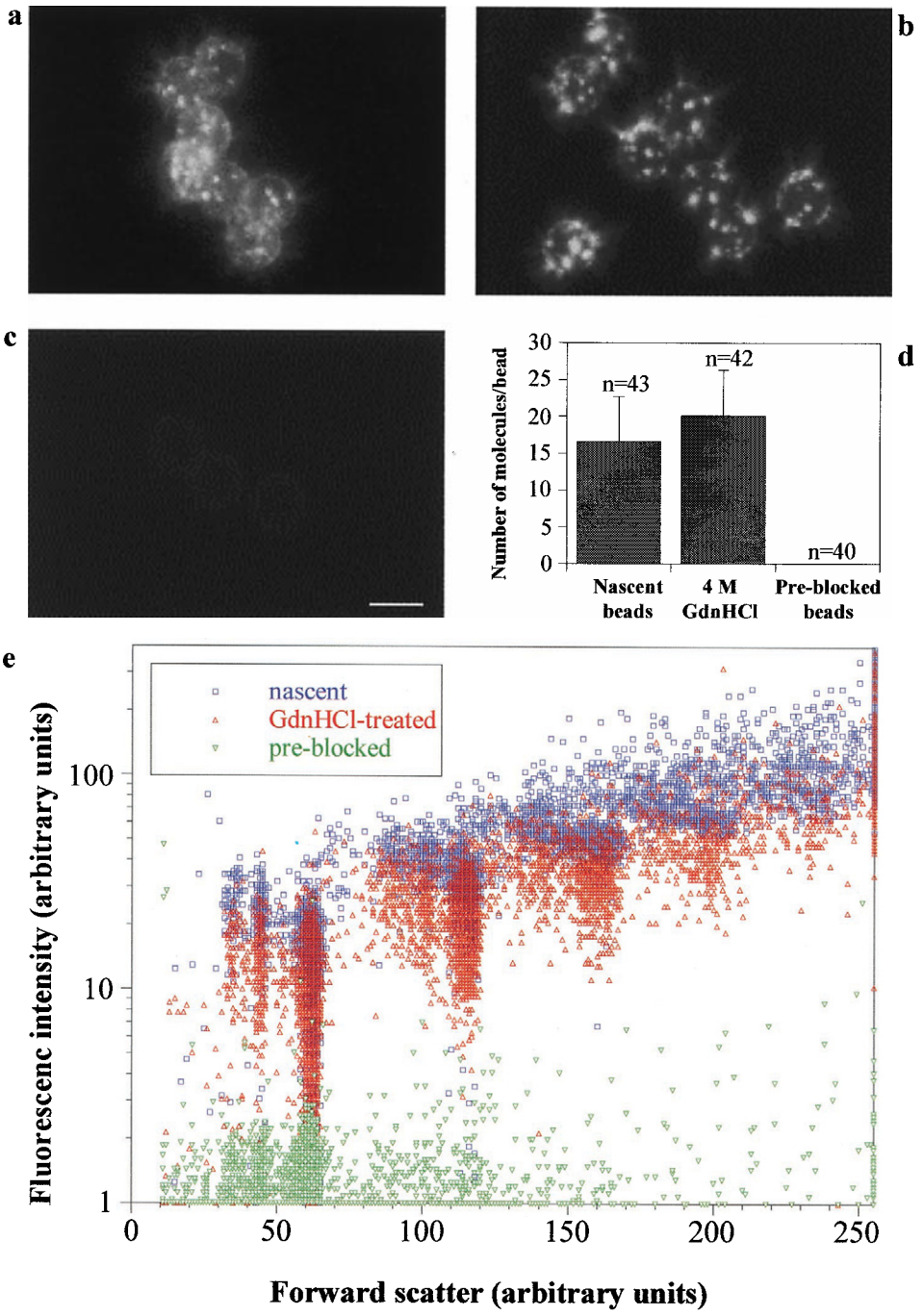

FIGURE 5 Confocal microscopic images of latex microspheres treated with fluorescently labeled titin under various conditions. (*a*) Nonspecific binding of titin to nascent, untreated microspheres. (*b*) Nonspecific binding of titin to nascent microspheres in the presence of 4 M GdnHCl. (*c*) Nonspecific binding of titin to microspheres pre-blocked with 1% BSA and 0.2% Tween-20. Fluorescently labeled titin molecules were identified as bright spots on the microsphere surface. Images were acquired at identical instrumental settings. Scale bar, 3 μm. (*d*) Statistics of the microsphere-adsorbed titin molecules. (*e*) FACS analysis of the microspheres treated with fluorescently labeled titin. The high-forward-scatter microsphere populations observed in the case of nascent beads and 4 M GdnHCl represent integer multiples of microspheres cross-linked via titin.

ble WLC behavior during stretch (Fig. 6 *b*), as well as the recovery of the stretch-curve following a ~4-min rest period (Fig. 6 *c*).

DISCUSSION

Titin molecules were repetitively stretched with optical tweezers to explore the mechanisms of molecular fatigue. Repeated stretch-release cycles to high forces revealed that molecular fatigue appears during stretch only in the low-force regime (0–25 pN) but not at forces above ~25 pN. Whereas above ~25 pN only random force variations occurred between consecutive mechanical cycles for a given end-to-end length, below ~25 pN the stretch force curves systematically shifted toward the release curve with each cycle (Fig. 1, *a* and *b*). Therefore, a given force was reached at progressively increasing end-to-end lengths, suggesting that by the beginning of each consecutive mechanical cycle the molecule became progressively longer. The progressive lengthening possibly involves a time- and therefore rate-

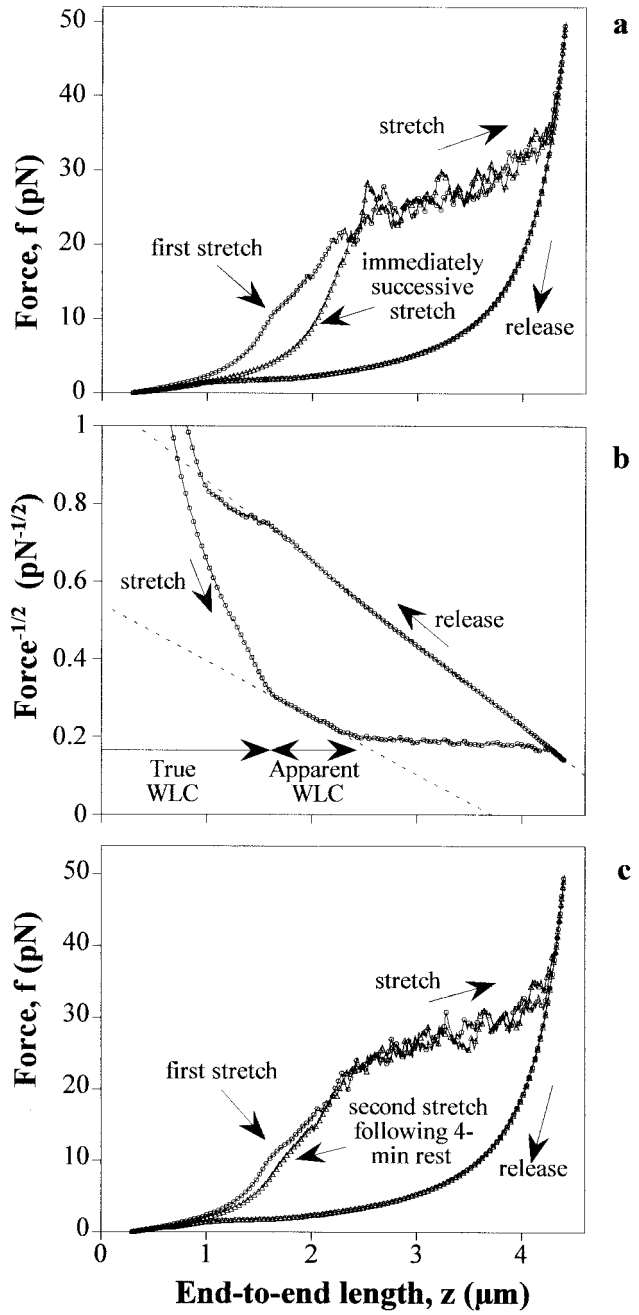

FIGURE 6 Monte Carlo simulation based on the intra-chain cross-link rupture/formation model. Arrows indicate direction of data acquisition (stretch or release). (*a*) The f versus z curves during first and the immediately following stretch-release cycles. (*b*) The $f^{-1/2}$ versus z curve of the first stretch-release cycle, revealing that the apparent, highly flexible WLC behavior is reproduced in the simulated data. (*c*) The f versus z curves during first stretch-release cycle and the cycle following a 4-min rest period.

dependent structural rearrangement in titin. Indeed, when stretching titin to $f_{max} < 25$ pN (Fig. 1 *c*), force hysteresis appeared, suggesting that the molecule is not in conformational equilibrium even in the low-force regime. The apparently reversible force curves seen in this low-force regime in our earlier work (Fig. 4A inset in Kellermayer et al., 1997) were probably collected on worn-out titin molecules, which explains the lack of force hysteresis in that data set. The stretch behavior recovered if the molecule was allowed to rest for minutes (>4 min) in the shortened, no-force (slack) or low-force state (Fig. 1 *d*). Thus, mechanical fatigue is a transition between shortened and lengthened states of the molecule, where the forward, or lengthening, reaction is relatively rapid (time constant on the order of tens of seconds) and strongly facilitated by external force, whereas the reverse, or shortening, reaction is slow (time constant on the order of minutes) and inhibited by force.

The structural transitions in the mechanically manipulated titin molecule leading to fatigue could derive from either 1) progressive unfolding of globular domains, 2) progressive dissociation of parts of the titin chain nonspecifically attached to the microsphere surface, or 3) a progressive disruption of chain-shortening, nonspecific intramolecular cross-links. Based on experimental and theoretical considerations it is unlikely that either progressive domain unfolding or nonspecific titin-microsphere interactions contribute to molecular fatigue. It has previously been suggested that mechanical wear-out in titin may result when, after mechanical unfolding, some of the domains fail to refold before the beginning of the consecutive stretch-release cycle, thus gradually increasing the ratio of unfolded/folded chain segments and thereby the apparent contour length (Kellermayer et al., 1997). Such a progressive unfolding was thought to be facilitated by the inhibition of domain refolding caused by the randomization of proline isoforms in the corners of the β-sheets of titin's globular domains (Kiefhaber et al., 1992). We tested the effect of progressive unfolding by modeling, with the WLC theory (Bustamante et al., 1994; Marko and Siggia, 1995), the mechanical behavior of a serially linked chain containing variable ratios of unfolded and folded segments and comparing the results with experimental data (Fig. 3). Progressive unfolding converts the short ($L \approx 1$ μm (Nave et al., 1989)) and stiff ($A \approx 15$ nm (Higuchi et al., 1993)) folded protein into the long ($L \approx 10$ μm (Labeit and Kolmerer, 1995)) and flexible ($A \approx 1.6$ nm (Kellermayer et al., 2000)) unfolded form. As a result, the apparent contour length, which entails the features of both the folded and unfolded segments, gradually increases, whereas the persistence length decreases. The longer the apparent contour length, the shorter the apparent persistence length. Such an opposite behavior of the contour and persistence lengths predicts that the extrapolated linear fits to the high-force regime in $f^{-1/2}$ versus z curves (Eq. 2, see Materials and Methods) corresponding to progressively unfolded titin pass through a common off-axis intersection (crossover point, Fig. 3 *a*), provided that there are no significant local deviations from the mean elastic behavior. In support of the prediction, extrapolated linear fits to the release force $f^{-1/2}$ data of a

titin strand (where the molecule is in conformational equilibrium (Kellermayer et al., 1997, 2000)) stretched to progressively increasing lengths do traverse a common off-axis intersection (Fig. 3 *b*). If the stretch behavior of titin involved merely a shift in the unfolded/folded ratio, then the extrapolated linear fit to the stretch force $f^{-1/2}$ data (before the onset of the unfolding transition) should also pass through this common intersection. By contrast, the linear fit to the stretch data failed to pass through the crossover point (Fig. 3 *b*). The *y* axis intercept of the stretch data describes a chain that is even more flexible than the completely unfolded polypeptide. Because chain flexibility exceeding that of the completely unfolded polypeptide is not physically realistic based purely on elasticity mechanisms, the highly flexible apparent WLC behavior seen during stretch is related to the nonequilibrium behavior of the molecule (Fig. 1 *c*) that involves the kinetics of chain-shortening associations. It is not inconceivable that partial refolding of globular domains, into β-hairpin structures, for example, may form such kinetic intermediates. However, β-hairpin structures fold in $\sim$6 μs at room temperature (Muñoz et al., 1997) in contrast to the minutes time scale for the re-establishment of molecular fatigue, and fatigue occurs even in lieu of prior domain unfolding (see Fig. 1 *c*). Nonspecific association of parts of the titin molecule to the microsphere surface could also, artificially, lead to mechanical fatigue. During stretch, such a titin molecule is gradually peeled off the bead surface, thereby increasing the apparent contour length. Nonspecific titin-microsphere interaction was tested by stretching titin in the presence of the chemical denaturant GdnHCl and by directly measuring the quantity of titin nonspecifically adsorbed to the microsphere surface under a variety of experimental conditions. The 4 M GdnHCl completely abolished titin's molecular fatigue (Fig. 4) but did not inhibit the nonspecific binding of titin to the microsphere surface (Fig. 5). Furthermore, the routine procedure of blocking the microspheres with 1% BSA and 0.2% Tween-20 very strongly inhibited the nonspecific binding of titin (Fig. 5). Although microsphere blocking may not completely rule out the presence of short-lifetime interactions, the experiments with GdnHCl demonstrate that molecular fatigue is not likely to be caused by transient titin-bead interactions. These control experiments were carried out for latex beads only. Therefore, the silica beads at the M-line end could, in principle, be implicated in artificially providing nonspecific binding sites. However, in titin stretching experiments where the silica bead was replaced with latex the results were identical to those obtained using silica. Thus, molecular fatigue was not influenced by the type of microsphere used. In sum, neither progressive domain unfolding nor nonspecific titin-microsphere interaction explains molecular fatigue.

To explain our experimental observations, we propose the following model. Titin's molecular fatigue derives from the kinetics of intra-chain interactions or bonds that shorten the molecule below its available contour length. The contour length is reduced by each bond according to the length of the molecule segment it encloses. Under force, the bonds rupture (forward reaction), which leads to a progressive increase of titin's apparent contour length. External force modulates the rate of bond rupture by reducing the bond energy barrier depending on the axial length change it induces along the reaction coordinate (Eq. 11). This length change is equivalent to the characteristic distance between the bond's ground and transition states along the bond dissociation reaction coordinate. In our experiments we stretched titin faster than the equilibrium bond rupture rate, meaning that the force generated in the molecule upon stretch increased faster than the rate of chain lengthening due to bond rupture. As a result, at a given extension, higher forces are measured when most of the bonds are in place (i.e., in the first stretch cycle) than when most of the bonds are broken (i.e., in subsequent stretch cycles; Fig. 1, *a* and *b*). In contrast to the forward reaction the bond re-forming reverse reaction is a slow, diffusion-driven process in which the segments of the shortened chain collide so that bond-forming counter-sites may find each other. Because the bond-forming reaction reduces the concentration of both counter-sites, the reaction proceeds with second-order kinetics (Eq. 9). Extending the chain axially dilutes the bond-forming counter-sites, thereby inhibiting the reverse reaction. The reaction will proceed with the maximum rate if the chain (or the involved chain segment) is held at a length equal to its free-solution equilibrium mean end-to-end distance. The Monte Carlo simulation based on this kinetic model reproduced the experimental observations (Fig. 6) indicating that our model qualitatively describes titin's molecular fatigue. The predictive power of the model is limited, however. The limitations arise from uncertainties in 1) the geometry of the internally cross-linked chain and the variation thereof from one mechanical cycle to the other, 2) the number and local density of bond-forming sites, and 3) how the structure of the chain and other factors (e.g., excluded volume effects and freely diffusible counterions) may influence binding-site accessibility. Furthermore, nonspecific side-side interactions between co-aligned segments of parallel-arranged titin molecules could, in principle, also lead to molecular fatigue of yet unpredictable magnitude. The development of a quantification for molecular fatigue may, in the future, result in the construction of more explicit models.

Molecular fatigue is particularly prominent at forces where the tandem globular domains in titin are nearly completely extended (but not unfolded) (Linke et al., 1996; Trombitás et al., 1998). Furthermore, if titin is kept in a partially extended (but low-force) state, where the tandem globular domains remain extended, molecular fatigue is re-established during rest (Fig. 1 *d*). Thus, the segments harboring cross-links are pre-unfolded or quasi-unfolded. The rest of the molecule (the native part that displays the

unfolding transition at higher forces) recovers on the time scale of the experiment. Although the exact nature of the nonspecific intra-chain bonds remains to be established, we speculate that they are electrostatic. In support of this idea, the dynamic stiffness of relaxed myofibrils has been previously shown to be ionic strength dependent (Linke et al., 1998). In addition, we have observed here (data not shown) that upon lowering the ionic strength the forces required to extend titin are significantly increased and often exceed the trapping force.

Titin's mechanical fatigue involves a segment of the molecule that behaves as an unfolded or pre-unfolded chain and provides an abundance of noncovalent binding sites. The PEVK segment, which has previously been shown to probably possess quasi-unfolded characteristics (Trombitás et al., 1998) and carries a preponderance of charged residues (Labeit and Kolmerer, 1995), may therefore be involved. Electrostatic interactions within the PEVK segment may shorten its apparent contour length, and the external force may increase the apparent contour length through the rupture of these bonds. Indeed, ionic-strength-dependent passive stiffness is greater in the case of titins expressing a longer PEVK segment (Linke et al., 1998). Alternatively, molecular fatigue could be caused by interactions between neighboring globular domains, in the form of metastable dimeric state, for example (Murray et al., 1995), provided that they lengthen through many intermediates and not in an all-or-none fashion (Rief et al., 1997). Transient electrostatic interactions within titin's A-band segment could, in principle, also lead to molecular fatigue. However, even in the case of short tethers that likely included the I-band segment only (Fig. 4 *a*), molecular fatigue was significant. Thus, although the A-band segment of titin may contribute to molecular fatigue, it is not the dominant component responsible for it.

If the cross-links do not re-form before the beginning of the subsequent stretch-release cycle, then the molecule remains longer than at the beginning of the preceding cycle. Thus, a length adjustment takes place that changes the molecule's length with a distance (Δl) that depends on the recent history of the mechanical perturbation: the maximum force and the stretch rate in the preceding cycle and the length of resting time. Notably, mechanical wear-out has recently been documented in single, isolated chromosomes (Houchmandzadeh and Dimitrov, 1999), suggesting that molecular fatigue may be a common characteristic of complex biopolymer systems. In striated muscle the length change associated with titin's molecular fatigue may have physiological significance. The thermodynamic disadvantage of not regaining the entire amount of the invested mechanical energy may serve a biological purpose. As shown by our results on passive single soleus muscle fibers (Fig. 2), fatigue is prevalent during repeated stretch-release cycles, and, when extrapolated to the single titin molecule, the process occurs in a force regime identical to that seen in the single-titin experiments. Molecular fatigue may be seen as an adaptive process in which the passive mechanical properties of striated muscle are adjusted according to recent mechanical history. The process could dynamically optimize the apparent contour length of titin's elastic segment through repeated contractile cycles. Furthermore, the kinetic determinants of the adjustable-length segment's force response may adjust the spring's apparent stiffness to the rate of mechanical perturbation: the faster the stretch, the stiffer the spring, and vice versa. Considering that the charge distribution along titin can vary as a function of cytosolic factors (e.g., pH, ionic strength, and divalent cations), the kinetic mechanism proposed herein provides means for the chemical modulation of muscle's apparent elasticity.

The T12 antibody was generously donated by D. O. Fürst. The help of László Grama with the FACS measurements is gratefully acknowledged. This work was supported by grants from the Hungarian Science Foundation (OTKA F025353) and the Hungarian Ministry of Health (ETT T-06–021/97) to M.S.Z.K., National Institutes of Health Heart, Lung, and Blood Institute (HL61497 and HL62881) to H.L.G., and by grants from the National Institutes of Health (GM-32543) and the National Science Foundation (MBC 9118482) to C.B. M.S.Z.K. is recipient of the Bolyai János Fellowship of the Hungarian Academy of Sciences, and H.L.G. is an established investigator of the American Heart Association.

REFERENCES

Bell, G. I. 1978. Models for the specific adhesion of cells to cells. *Science.* 200:618–627.

Bustamante, C. J., J. F. Marko, E. D. Siggia, and S. B. Smith. 1994. Entropic elasticity of λ-phage DNA. *Science.* 265:1599–1600.

Cazorla, O., A. Freiburg, M. Helmes, T. Centner, M. McNabb, K. Trombitás, S. Labeit, and H. Granzier. 2000. Differential expression of cardiac titin isoforms and modulation of cellular stiffness. *Circ. Res.* 86:59–67.

Chase, P. B., and M. J. Kushmerick. 1988. Effects of pH on contraction of rabbit fast and slow skeletal muscle fibers. *Biophys. J.* 53:935–946.

Eisenberg, B. 1983. Quantitative ultrastructure of mammalian skeletal muscle. *In* Handbook of Physiology, Skeletal Muscle. American Physiological Society, Bethesda, MD. 73–113.

Evans, E., and K. Ritchie. 1997. Dynamic strength of molecular adhesion bonds. *Biophys. J.* 72:1541–1555.

Fürst, D. O., M. Osborn, R. Nave, and K. Weber. 1988. The organization of titin filaments in the half-sarcomere revealed by monoclonal antibodies in immunoelectron microscopy: a map of ten nonrepetitive epitopes starting at the Z line extends close to the M line. *J. Cell Biol.* 106: 1563–1572.

Granzier, H. L. M., M. Helmes, and K. Trombitás. 1996. Nonuniform elasticity of titin in cardiac myocytes: a study using immunoelectron microscopy and cellular mechanics. *Biophys. J.* 70:430–442.

Granzier, H. L. M., and T. Irving. 1995. Passive tension in cardiac muscle: the contribution of collagen, titin, microtubules and intermediate filaments. *Biophys. J.* 68:1027–1044.

Granzier, H. L., and K. Wang. 1993a. Gel electrophoresis of giant proteins: solubilization and silver-staining of titin and nebulin from single muscle fiber segments. *Electrophoresis.* 14:56–64.

Granzier, H. L. M., and K. Wang. 1993b. Passive tension and stiffness of vertebrate skeletal and insect flight muscles: the contribution of weak cross-bridges and elastic filaments. *Biophys. J.* 65:2141–2159.

Gregorio, C. C., H. Granzier, H. Sorimachi, and S. Labeit. 1999. Muscle assembly: a titanic achievement? *Curr. Opin. Cell Biol.* 11:18–25.

Helmes, M., K. Trombitás, T. Centner, M. S. Z. Kellermayer, S. Labeit, W. A. Linke, and H. Granzier. 1999. Mechanically driven contour-length adjustment in rat cardiac titin's unique N2B sequence: titin is an adjustable spring. *Circ. Res.* 84:1339–1352.

Higuchi, H., Y. Nakauchi, K. Maruyama, and S. Fujime. 1993. Characterization of beta-connectin (titin 2) from striated muscle by dynamic light scattering. *Biophys. J.* 65:1906–1915.

Horowits, R. 1992. Passive force generation and titin isoforms in mammalian skeletal muscle. *Biophys. J.* 61:392–398.

Horowits, R., E. S. Kempner, M. E. Bisher, and R. J. Podolsky. 1986. A physiological role for titin and nebulin in skeletal muscle. *Nature.* 323:160–164.

Horowits, R., and R. J. Podolsky. 1987. The positional stability of thick filaments in activated skeletal muscle depends on sarcomere length: evidence for the role of titin filaments. *J. Cell Biol.* 105:2217–2223.

Houchmandzadeh, B., and S. Dimitrov. 1999. Elasticity measurements show the existence of thin rigid cores inside mitotic chromosomes. *J. Cell Biol.* 145:215–223.

Kazmirski, S. L., and V. Daggett. 1998. Non-native interactions in protein folding intermediates: molecular dynamics simulations of hen lysozyme. *J. Mol. Biol.* 284:793–806.

Kellermayer, M. S. Z., and H. L. M. Granzier. 1996. Calcium dependent inhibition of in vitro thin-filament motility by native titin. *FEBS Lett.* 380:281–286.

Kellermayer, M. S. Z., S. B. Smith, C. Bustamante, and H. L. Granzier. 1998. Complete unfolding of the titin molecule under external force. *J. Struct. Biol.* 122:197–205.

Kellermayer, M. S. Z., S. Smith, C. Bustamante, and H. L. Granzier. 2000. Mechanical manipulation of single titin molecules with laser tweezers. *In* Elastic Filaments of the Cell. H. L. Granzier and G. H. Pollack, editors. Kluwer Academic Press, Seattle.

Kellermayer, M. S. Z., S. B. Smith, H. L. Granzier, and C. Bustamante. 1997. Folding-unfolding transitions in single titin molecules characterized with laser tweezers. *Science.* 276:1112–1116.

Kiefhaber, T., H. Kohler, and F. Schmid. 1992. Kinetic coupling between protein folding and prolyl isomerization. *J. Mol. Biol.* 224:217.

Labeit, S., and B. Kolmerer. 1995. Titins: giant proteins in charge of muscle ultrastructure and elasticity. *Science.* 270:293–296.

Linke, W. A., M. Ivemeyer, P. Mundel, M. R. Stockmeier, and B. Kolmerer. 1998. Nature of PEVK-titin elasticity in skeletal muscle. *Proc. Natl. Acad. Sci. U.S.A.* 95:8052–8057.

Linke, W. A., M. Ivemeyer, N. Olivieri, B. Kolmerer, J. C. Ruegg, and S. Labeit. 1996. Towards a molecular understanding of the elasticity of titin. *J. Mol. Biol.* 261:62–71.

Linke, W. A., V. I. Popov, and G. H. Pollack. 1994. Passive and active tension in single cardiac myofibrils. *Biophys. J.* 67:782–792.

Marko, J. F., and E. D. Siggia. 1995. Stretching DNA. *Macromolecules.* 28:8759–8770.

Maruyama, K. 1997. Connectin/titin, giant elastic protein of muscle. *FASEB J.* 11:341–345.

Merkel, R., P. Nassoy, A. Leung, K. Ritchie, and E. Evans. 1999. Energy landscapes of receptor-ligand bonds explored with dynamic force spectroscopy. *Nature.* 397:50–53.

Muñoz, V., P. A. Thompson, J. Hofrichter, and W. A. Eaton. 1997. Folding dynamics and mechanism of β-hairpin formation. *Nature.* 390:196–199.

Murray, A. J., S. J. Lewis, A. N. Barclay, and R. L. Brady. 1995. One sequence, two folds: a metastable structure of CD2. *Proc. Natl. Acad. Sci. U.S.A.* 92:7337–7341.

Nave, R., D. O. Fürst, and K. Weber. 1989. Visualization of the polarity of isolated titin molecules: a single globular head on a long thin rod as the M band anchoring domain? *J. Cell Biol.* 109:2177–2187.

Ogut, O., H. L. Granzier, and J.-P. Jin. 1999. Acidic and basic troponin T isoforms in mature fast-twitch skeletal muscle and effect on contractility. *Am. J. Physiol.* 276:C1162–C1170.

Rief, M., M. Gautel, F. Oesterhelt, J. M. Fernandez, and H. E. Gaub. 1997. Reversible unfolding of individual titin immunoglobulin domains by AFM. *Science.* 276:1109–1112.

Rief, M., M. Gautel, A. Schemmel, and H. E. Gaub. 1998. The mechanical stability of immunoglobulin and fibronectin III domains in the muscle protein titin measured by atomic force microscopy. *Biophys. J.* 75: 3008–3014.

Smith, S. B., Y. Cui, and C. Bustamante. 1996. Overstretching B-DNA: the elastic response of individual double-stranded and single-stranded DNA molecules. *Science.* 271:795–799.

Soteriou, A., M. Gamage, and J. Trinick. 1993. A survey of interactions made by the giant protein titin. *J. Cell Sci.* 104:119–123.

Trinick, J. 1996. Cytoskeleton: titin as a scaffold and spring. *Curr. Biol.* 6:258–260.

Trinick, J., and L. Tskhovrebova. 1999. Titin: a molecular control freak. *Trends Cell Biol.* 9:377–380.

Trombitás, K., M. Greaser, S. Labeit, J.-P. Jin, M. Kellermayer, M. Helmes, and H. Granzier. 1998. Titin extensibility in situ: entropic elasticity of permanently folded and permanently unfolded molecular segments. *J. Cell Biol.* 140:853–859.

Trombitás, K., J.-P. Jin, and H. L. Granzier. 1995. The mechanically active domain of titin in cardiac muscle. *Circ. Res.* 77:856–861.

Tskhovrebova, L., J. Trinick, J. A. Sleep, and R. M. Simmons. 1997. Elasticity and unfolding of single molecules of the giant muscle protein titin. *Nature.* 387:308–312.

Wang, K. 1996. Titin/connectin and nebulin: giant protein rulers of muscle structure and function. *Adv. Biophys.* 33:123–134.